

Effect of source temperature on the electrical transport, microstructural and optical properties of tin monosulfide thin films prepared by close spaced sublimation method

Ng Wongcharoen* and T Gaewdang

Physics Department, King Mongkut's Institute of Technology Ladkrabang, Bangkok 10520, Thailand

*Email: ngamnit.wo@kmitl.ac.th

Abstract. Tin monosulfide (SnS) thin films were prepared by close spaced sublimation method at three different source temperatures of 550, 575 and 600°C. Structural, textural and compositional features were investigated by XRD, SEM, EDS and Raman spectroscopy. From absorption spectra, direct band gap increased from 1.18 to 1.23 eV with increasing source temperature. Electrical resistivity, Hall constant, carrier concentration and mobility values of the films prepared at source temperature of 600°C were 0.54 Ω.cm, 40.76 cm³/C, 1.53x10¹⁷ and 75.48 cm²/(V.s), respectively. The temperature-dependent conductivity was performed in the temperature range of 50-300 K. It was shown that three types of conduction mechanisms can be expected: thermionic emission passing through grain boundary at high temperature range (240-300 K), the Mott variable-range hopping (Mott-VRH) at low temperature range (135-235 K) and the Efros-Shklovskii variable-range hopping (ES-VRH) at very low temperature range (80-130 K).

1. Introduction

In the past years thin films of SnS have attracted much attention because of their potential applications in the fabrications of photovoltaic, solar cells and optoelectronic devices [1]. SnS is a potential absorber of solar cell because of its high optical absorption coefficient above the photon energy threshold of 1.3 eV, which is close to the optimal band gap. Moreover, SnS shows intrinsic p-type conductivity with carrier concentrations in the range 10¹⁶-10¹⁸ cm⁻³, which is suitable for absorber of solar cell. In addition, both Sn and S are abundant in nature and non-toxic. The latter characteristics are very important for photovoltaic industry with the currently available CdTe and CuInSe₂ materials, although they do also exhibit high efficiencies. SnS thin films can be prepared by a variety of methods [2]. Among these methods, close spaced sublimation method is proposed low consumed materials, high growth rate, ease to control stoichiometric composition and ease to extend to large scale production [3, 4]. In this study, we prepared SnS thin films on glass substrate by close spaced sublimation method in vacuum. Influence of different source temperatures on structural, optical and electrical properties of SnS films was investigated.



2. Materials and methods

SnS thin films were prepared on glass substrates by close spaced sublimation method using a home-made apparatus. Three different source temperatures (T_s) as 550, 575 and 600°C were used to prepare SnS thin films. The deposition time was 10 min. The glass substrate temperature was fixed at lower than source temperature around 100°C by PID temperature controller. The crystal structure of these films was checked by X-ray diffraction technique with a Bruker D 8 diffractometer using CuK_α radiation. Surface morphology was examined by LEO1455VP scanning electron microscope. The elemental composition was analyzed by using EDS. Raman spectroscopy was performed by Renishaw inVia micro-Raman microscope. The optical absorption spectra were measured with a UV-Vis spectrophotometer in the 400-1000 nm wavelength range. Electrical properties of the films were evaluated by Hall effect and resistivity measurements in the van der Pauw configuration at room temperature. The temperature-dependent conductivity of SnS thin films was measured by two probe method. The cryogenic system with a He closed cycle allows us to measure electrical conductivity of the films from 50 to 300 K.

3. Results and discussion

3.1. Structural analysis

The XRD patterns of SnS films deposited at three different source temperatures of 550, 575 and 600 °C are shown in Figure 1. All samples belonged to orthorhombic structure corresponding to file JCPDS 73-1859 with preferred orientation (400) plane. The variation of lattice parameters with source temperature is shown in Figure 2. The parameter “a” increased significantly attain a maximum value at source temperature of 575°C and above this source temperature, parameter “a” was rather constant. The small variation of lattice parameter “a” is probably the result of the strain especially in direction perpendicular to substrate. The parameter “b” and “c” are more or less constant with the increase of source temperature. The biggest texture coefficient value [5] about 2.11 was observed in the films prepared at source temperature of 600°C. Figure 3 shows SEM images of SnS films grown at different source temperatures. The films contained rectangular plate-like form with dimension around 12.5 μm in length and 1.5 μm in thickness was observed in the films prepared at source temperature of 600°C.

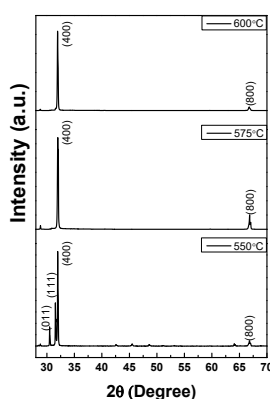


Figure 1. XRD patterns of SnS thin films prepared at different source temperatures.

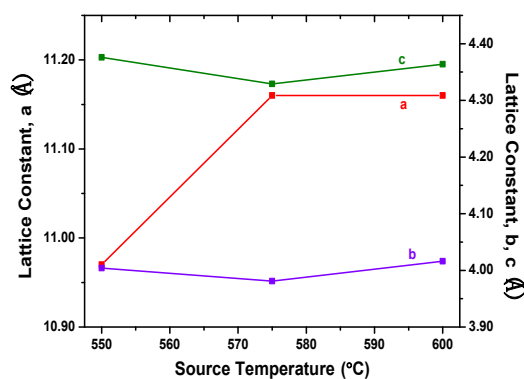


Figure 2. Variation of lattice constant values as a function of source temperature.

From EDS analysis, the relative atomic percentages of Sn and S in the films prepared with source temperature 600°C were 51.21% and 48.79 %, respectively. For all three typical films, only one Raman peak located around 220 cm^{-1} was presented in Figure 4. This Raman peak was attributed to LO phonon mode of SnS phase [6]. Regarding to the peak intensity, it suggested that the films prepared at source temperature of 600°C revealed the best crystal quality due to the strongest peak intensity.

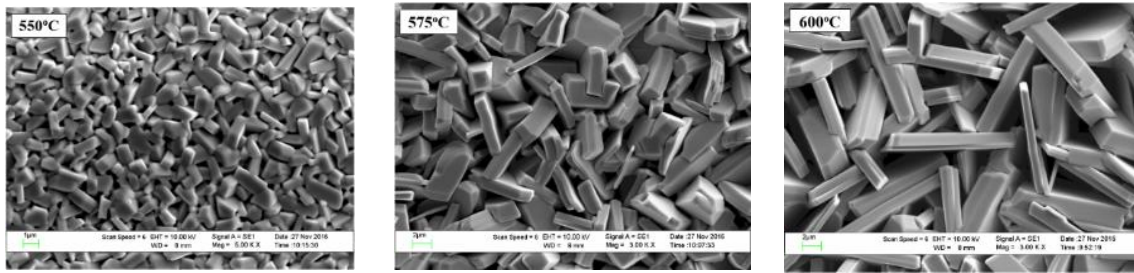


Figure 3. SEM images of SnS thin films prepared at different source temperatures.

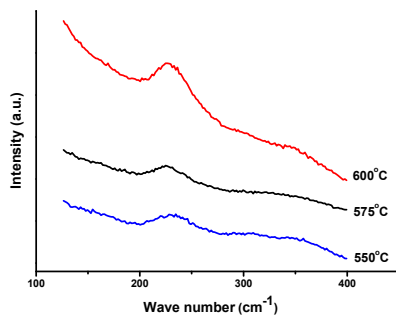


Figure 4. Raman spectra of SnS thin films prepared at different source temperatures.

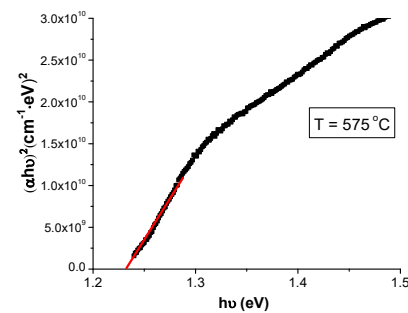


Figure 5. Plot of $(\alpha hv)^2 = A(hv - E_g)$ of SnS thin films prepared at source temperature of 600°C.

3.2. Optical properties

From Figure 5, the plot of $(\alpha hv)^2 = A(hv - E_g)$ of SnS films prepared at source temperature 600°C revealed the straight-line nature indicating that the optical transition in the films is direct allowed transition and the $h\nu$ -axis interception resulting the band gap value. The band gap was found to increase from 1.18 to 1.23 eV when the source temperature increased from 550°C to 600°C.

3.3. Electrical properties

Electrical properties of the films were evaluated by Hall effect and resistivity measurements in the van der Pauw configuration. The positive sign of the Hall coefficient confirmed p-type conductivity in all studied films. The lowest resistivity and highest carrier concentration values were observed on the films prepared at source temperature of 600 °C. Resistivity, Hall constant, carrier concentration and mobility values of the films were 0.54 Ω .cm, 40.76 cm^3/C , 1.53×10^{17} and 75.48 $\text{cm}^2/(\text{V.s})$, respectively. The obtained results are in agreement with the reported literatures [1,3,7]. Figure 6 (a) shows the Arrhenius plot of $\ln(\sigma)$ and $1000/T$ for the films prepared with source temperature of 600°C. As seen in Figure 6 (a), no single mechanism can be fitted in the whole curve of conductivity. At high temperature, the electrical conductivity of the sample is dominated by thermal activation passing through grain boundaries. The temperature dependence of the electrical conductivity of the films was firstly analyzed using Seto's model as the following relation [8]:

$$\ln\left(\sigma T^{1/2}\right) = -\frac{E_a}{k}\left(\frac{1}{T}\right) + \ln \sigma_0 \quad (1)$$

where σ_0 is pre-exponential factor, k is Boltzmann's constant and E_a is the activation energy. This model related to grain boundaries which trap carriers and the barrier height value appeared. As shown in Figure 6 (b), a good linear relationship can be observed in the Arrhenius plot in the high temperature range (240-300 K). The important parameters deduced from Seto's model were listed in Table 1: L is crystallite size, E_b is barrier height, N_a is acceptor concentration, E_t is trap energy level,

N_t is trap concentration and L_D is Debye length. Figure 6 (c) shows the plot of $\ln(\sigma T^{1/2})$ vs $T^{-1/4}$. The plot was found to be linear at temperature range of 135-235K. This suggested that the conduction is controlled by Mott variable-range hopping (Mott-VRH) instead of the Seto's model at high temperature. The Mott's parameters can be extracted from the relation [8]:

$$\ln(\sigma T^{1/2}) = -\left(\frac{T_{0,Mott}}{T}\right)^{1/4} + \ln \sigma_{0,Mott} \tag{2}$$

The important parameters deduced from Mott-VRH model were tabulated in Table 2: $T_{0,Mott}$ is a characteristic temperature coefficient, $\sigma_{0,Mott}$ is pre-exponential factor, $N_0(E_F)$ is density of state at the Fermi level, $R_{hop, Mott}$ is average hopping distance, and $W_{hop, Mott}$ is average hopping energy. At very low temperature range (80-130 K), the measured data were satisfied the Efros-Shklovskii variable-range hopping (ES-VRH). In this electrical conduction mechanism region, the electron interaction caused the density of state at Fermi level is separated and became to the coulomb gap (Δ_C). The conductivity in ES-VRH model is given as [8]

$$\ln(\sigma T) = -\left(\frac{T_{0,ES}}{T}\right)^{1/2} + \ln \sigma_{0,ES} \tag{3}$$

Figure 6 (d) shows the plot of $\ln(\sigma T)$ vs $T^{-1/2}$. The important parameters deduced from ES-VRH model were listed in Table 3: $T_{0,ES}$ is a characteristic temperature coefficient, $\sigma_{0,ES}$ is pre-exponential factor, $R_{hop, ES}$ is average distance and $W_{hop, ES}$ is average hopping energy.

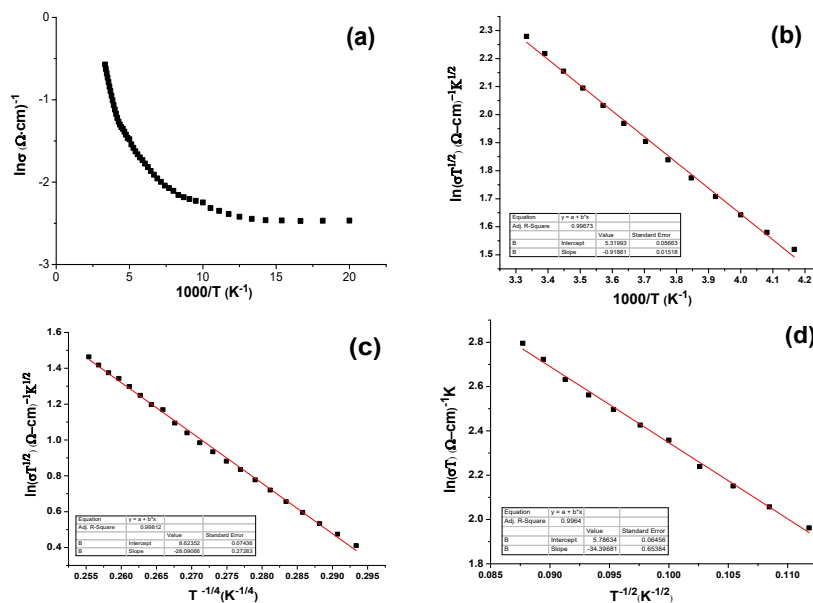


Figure 6. $\ln(\sigma)$ vs $1000/T$ plot, (b) $\ln(\sigma T^{1/2})$ vs $1000/T$ plot, (c) $\ln(\sigma T^{1/2})$ vs $T^{-1/4}$ plot and (d) $\ln(\sigma T)$ vs $T^{-1/2}$ plot of SnS thin films prepared at source temperature of 600°C.

Table 1. Seto's parameters at high temperature of the films prepared at source temperature 600°C.

Temperature range	E_g (eV)	ϵ_r	L (nm)	E_b (eV)	N_a (cm ⁻³)	E_t (eV)	N_t (cm ⁻²)	L_D (nm)
240-300	1.23	10.65	47.30	0.0792	1.67×10^{17}	0.527	7.90×10^{11}	9.07

Table 2. Mott's parameters at low temperature of the films prepared at source temperature 600°C.

Temperature range	$\sigma_{0,Mott}$ (S/cm)	$T_{0,Mott}$ (K)	ξ_{Mott} (nm)	$N_0(E_F)$ ($\text{cm}^{-3} \cdot \text{eV}^{-1}$)	$R_{hop,Mott}$ (nm)	$\frac{R_{hop,Mott}}{\xi_{Mott}}$	$W_{hop,Mott}$ (meV)
135-235	5.56×10^3	6.23×10^5	0.806	6.39×10^{20}	2.29	2.84	31.06

Table 3. ES's parameters at very low temperature of the films prepared at source temperature 600°C.

Temperature range	$\sigma_{0,ES}$ (S/cm)	$T_{0,ES}$ (K)	$R_{hop,ES}$ (nm)	ξ_{ES} (nm)	$\frac{R_{hop,ES}}{\xi_{ES}}$	$W_{hop,ES}$ (meV)	Δ_C (eV)
80-130	3.25×10^2	1.18×10^3	39.10	46.56	0.84	15.20	3.76×10^{-6}

4. Conclusions

Influence of source temperature on microstructure, optical and electrical properties of SnS films prepared by close spaced sublimation method in vacuum was investigated. XRD analysis results indicated that all studied films belonged to orthorhombic structure. Raman spectra of the all three typical films presented the LO phonon mode. The band gap was found to increase from 1.18 to 1.23 eV when the source temperature increased from 550 to 600°C. The lowest resistivity and highest carrier concentration values were observed on the films prepared at source temperature of 600 °C. In the temperature range of 50-300 K, it was shown that three types of conduction mechanisms can be expected in the films prepared at source temperature of 600°C: thermionic emission across grain boundary at high temperature range (240-300 K), the Mott variable-range hopping (Mott-VRH) at low temperature range (135-235 K) and the Efros-Shklovskii variable-range hopping (ES-VRH) at very low temperature range (80-130K).

Acknowledgments

This work is supported by King Mongkut's Institute of Technology Ladkrabang (KMUTL) under grant number A118-0360-005.

References

- [1] Kumar K K, Manohari A, Dhanapandian S and Mahalingam T 2014 *Mater. Lett.* **131** p 167
- [2] Bashkurov S A, Gremenok V F and Ivanov V A 2011 *Semiconductor* **45(6)** p 749
- [3] Yanuar Y, Guastavino F, Llinares C, Djessas K and Massc G 2000 *J. Mater. Sci.* **19** p 2135
- [4] Zhan X, Shi C, Shen X, Yao M and Zhang Y 2012 *Adv. Mater. Res.* **590** p 148
- [5] Pan L L, Li G Y and Lian J S 2013 *Appl. Surf. Sci.* **274** p 365
- [6] Yang Y B, Dash J K, Xiang Y, Wang Y, Shi J, Dinolfo P H, Lu T M and Wang G C 2016 *J. Phys. Chem. C* **120** p 13199
- [7] Vidal J, Lany S, d'Avezac M, Zunger A, Zakutayev A, Francis J and Tate J 2012 *Appl. Phys. Lett.* **100** 032104
- [8] Baqiah H, Ibrahim N B, Abdi M H and Halim S A 2013 *J Alloys Compd.* **575** p 198